PRESSURE DROP ACROSS MICRO-PIN HEAT SINKS UNDER BOILING CONDITIONS

Ali Koşar°, Mehmed R. Özdemir*, Mehmet Keskinöz+,

°Faculty Member, Sabancı University, Faculty of Engineering and Natural Sciences, Mechatronics Engineering Program, Orhanlı, Tuzla, 34956, Istanbul, *Graduate Student, Sabancı University, Faculty of Engineering and Natural Sciences, Mechatronics Engineering Program, Orhanlı, Tuzla, 34956, Istanbul, +Faculty Member, Sabancı University, Faculty of Engineering and Natural Sciences, Electronics Engineering Program, Orhanlı, Tuzla, 34956, Istanbul

ABSTRACT

Two-phase pressure drop was studied in four different micro pin fin heat sinks. Micro pin fin heat sinks used in the current studies were operated under boiling conditions using water and R-123 as working fluids. It was observed that once boiling was initiated severe temperature fluctuations and flow oscillations were recorded for three of the micro pin fin heat sinks, which was characterized as unstable boiling. Pressure drop signals were presented just before and after the unstable boiling conditions. Flow images and FFT (fast Fourier Transform) profiles of pressure signals were used to explain experimental results and unstable nature in flow boiling observed in the three of the devices. Stable boiling conditions where the temperature and pressure drop had a steady and stable profile could be only obtained from one micro pin fin heat sink at high mass velocities. The two-phase pressure drop in this hydrofoil-based micro pin fin heat sink has been investigated using R-123 as the working fluid. Two-phase frictional multipliers have been obtained over mass fluxes from 976 to 2349 kg/m^2. It has been found that the two-phase frictional multiplier is strongly dependent on flow pattern. The theoretical prediction using Martinelli parameter based on the laminar fluid and laminar gas flow represented the experimental data fairly well for the spray-annular flow. For the bubbly and wavy-intermittent flow, however, large deviations from the experimental data were recorded. The Martinelli parameter was used successfully to determine the flow patterns, which were bubbly, wavy-intermittent, and spray-annular flow in the current study.

INTRODUCTION

The design of miniature devices using microfabrication techniques opens new opportunities in the science of thermal engineering, but requires in-depth understanding of the pertaining heat and fluid flow. To fill the lack of knowledge in micro scale convective flow, extensive research has been focused first on microchannels, which extended the knowledge about single-phase and flow boiling heat transfer and pressure drop. Reviews on heat and fluid flow in microchannels are now widely available in numerous archival publications [Mehendale et al. (2000), Palm (2001), Kandlikar (2002), Beergles et al. (2003), Garimella and Singhal (2004), Kandlikar (2004), Kandlikar and Grande (2004), Thome (2004)].

To augment the thermal performance of microchannels pin fin heat sinks were proposed by several investigators [Colgan et al. (2005), Qu et al. (2005), Prasher et al. (2006), Koşar and Peles (2006a), Koşar and Peles (2006b)], primarily for single-phase flows. Recently the study of heat transfer in micro pin fin heat sinks has been extended to flow boiling by Koşar and Peles (2006c), who studied boiling heat transfer in a hydrofoil-based micro pin fin heat sink and discussed boiling heat transfer mechanisms.

Two-phase pressure drop characteristics have been previously investigated for tube bundles consisting of long tubes (H/D>4) [Grant et al. (1979), Schrage et al. (1988), Dowlati and Kawaji (1999), Dowlati et al. (1996), Dowlati et al. (1990), Xu et al. (1998)]. The existing studies provide valuable knowledge on the two-phase pressure drop in conventional tube bundles. However, it is debatable to apply the prediction tools developed for circular long tubes to micro pin fins, which have a smaller H/d ratio (H/d<4), since there exists no study investigating diabatic two-phase pressure drop in short pin fin heat sinks in literature, whereas there exists only one study investigating two-phase pressure drop in circular micro pillars under adiabatic conditions (Krishnamurthy and Peles (2007)). Moreover, microfabrication technology enables the formation of unconventional pin fin geometries, which may reduce the pressure losses, and thus, may enhance thermal-hydraulic performance. No experimental data are present for those unconventional geometries (e.g. hydrofoil-based pin fins) in macro scale because of their expensive fabrication cost by standard manufacturing techniques. This lack of information provokes the need for research on flow across unconventional geometries in micro scale, so that designs of second generation micro heat exchangers would be successfully accomplished. The current study addresses to this issue with a hydrodynamic perspective and aims at providing insight into two-phase pressure drop across micro pin fin heat sinks. For this, four different micro pin fin heat sinks were tested under boiling conditions and using two different working fluids (water, R-123). This study includes the presentation of the pressure drop data from these devices under both unstable and stable boiling conditions and its detailed discussion.

DEVICE OVERVIEW

A Computer Aided Design (CAD) image of a representative device consisting of a 1800-μm wide and 1 cm long microchannel of depth 243-μm is shown in Fig. 1. In order to minimize ambient heat losses an air gap is formed on the two ends of the side walls, and an inlet and exit plenum, 4 mm long each, are etched on the thin silicon substrate (~150 μm). A heater, which serves as a thermistor for temperature

measurements, is deposited on the backside to deliver the heating power. A Pyrex cover seals the device from the top and allows flow visualization. Pressure taps are present at the inlet and exit of the device to enable pressure measurements. A representative micro pin fin heat sink is displayed in Fig. 1. The devices tested in this study are summarized in Table 1.

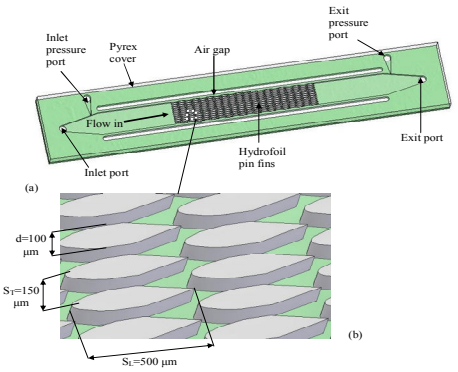

Fig. 1. (a) CAD model of the micro pin fin heat sink (b) Zoom in to the micro pin fins.

EXPERIMENTAL SETUP AND PROCEDURE

Experimental Setup

In Fig. 2, a schematic of the experimental setup is shown. The details about the experimental setup are included in the previous work of Koşar and Peles (2006c). The micro pin fin device was packaged by sandwiching it between two plates. The fluidic seals were forged using miniature "o-rings" while external electrical connections to the heater were provided from beneath through spring-loaded pins, which connected the heater to electrical pads residing away from the main micro pin fin device body. Resistance, pressure, and flow measurements were taken at a fixed flow rate in the loop.

Experimental Procedure

R-123 and de-ionized water were utilized as the working fluid in the experiments under the exit pressure of 101-539 kPa. First, the flow rate was fixed at the desired value, and data was taken after a steady flow rate had been obtained, while exit pressure was kept constant. Prior to acquiring experimental data the flow meter reading was adjusted to the desired flow rate. To obtain two-phase pressure data, voltage was applied in 0.5 volt increments across the heater, and the current/voltage data was recorded while ensuring the constancy of the flow rate, and pressures at the inlet and exit ports of the micro pin fin device were acquired at that each data point. The same procedure was repeated for other flow rates.

The uncertainties of the measured values, which are provided in Table 2, were obtained from manufacturer's specification sheets, while the uncertainties of the derived parameters were calculated using the method developed by Kline and McClintock (1953).

Device number	Working fluid	Pin shape	Pin configuration	S_T (μm)	S_L(μm)
1CRUB	R-123	Circular	Staggered	150	150
2CWUB	Water	Circular	Staggered	150	350
3HWUB	Water	Hydrofoil	Staggered	300	500
4HRSB	R-123	Hydrofoil	Staggered	150	500

Table 1. Devices tested in the current study

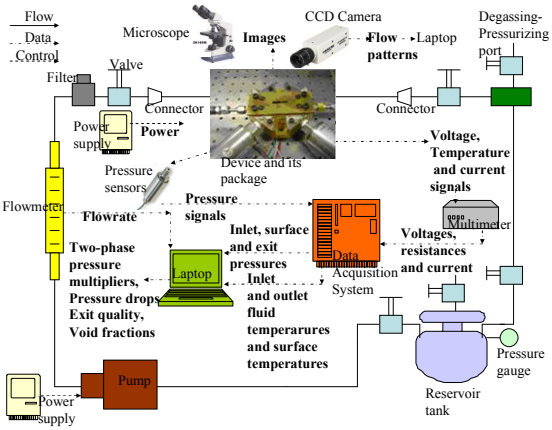

Fig. 2. Experimental setup.

Uncertainty	Error
Mass flux, G (for each reading)	1.0%
Pressure Readings (for the range)	0.25%
x_e	5%
Φ_L^2	2.5 %
Ambient temperature	0.1ºC
Electrical power, P	0.7%
Average temperature, $\overline{T}$	0.5 ºC

Table 2. Uncertainty data from the experiment.

RESULTS AND DISCUSSION

Two-phase pressure drop for configurations leading to unstable boiling

a) Pressure fluctuations

In the devices and configurations leading to unstable boiling (1 CRUB, CWUB, HWUB), a meager increase in heat flux triggers an abrupt and intense boiling with considerable increase in the surface temperature and pressure drop marking the arrival of flow instabilities at boiling inception. Boiling conditions are accommodated with significant flow, pressure, and temperature oscillations and are characterized as unstable boiling. The change in pressure drop with time gives necessary means to investigate the pressure fluctuations caused by flow instabilities. A potential source for pressure fluctuations would be these flow instabilities.

Figures 3a and b show the pressure fluctuations with time just before the unstable boiling starts in device 1CRUB at G=576 and 887 kg/m^{2}s. It can be noticed that there are no significant pressure fluctuations with the respect to time averaged pressure drop ($\Delta p'_{max}$~0.5kPa). This profile also prevails after unstable boiling initiates, and peak to peak

pressure drop fluctuations remain small compared to the time averaged pressure drop (Figs. 4 a and b), which is in contrast to the (Critical Heat Flux) CHF or premature CHF condition in microchannels in parallel, at which significant pressure fluctuations were reported in the literature [Kandlikar (2002)]. This implies that the mechanism behind unstable boiling in micro pin fin heat sinks is different from the CHF condition in microchannels, where the bubbles having the same size as the channel move back and forth along the microchannels causing fluctuations in flow, which result in pressure fluctuations.

In order to reveal the differences between pressure drops in unstable and stable boiling, FFTs (Fast Fourier Transform) of pressure fluctuations were taken. Thus, to analyze the signal behavior before and after unstable boiling, FFT profiles of the signals are used to see their energy spreads over the frequency. For this analysis, FFT sizes were taken as 2000, which corresponds to a frequency band of 500 Hz since the sampling periods between time domain samples were 10^{-3}s. First observation from Figs. 5 and 6 is that the peaks of the spectrum increase by a factor of 5.43, 8.54 and 4.33 for G=329, 576 and 887 kg/m^{2}s, respectively. This clearly indicates a drastic change in the pressure signals with the initiation of unstable boiling and a sharp increase in the energy peaks of the FFT profiles is apparent. Moreover, the mean of the magnitude spectrum on the side-lobes was also considered for each case. To perform this analysis, the windowed spectrum is used as illustrated in Fig. 6a, where W was taken as 120, and the windowing was done 30 samples before and after the peak. Thereafter, the ratio of the mean of the magnitude spectrum after unstable boiling to the mean of the magnitude spectrum before unstable was calculated for G=329, 576 and 887 kg/m^{2}s as 6.83, 6.38 and 4.28, respectively. These findings suggest that not only the spectrum peak increases significantly but the side-lobe energy also gets drastically higher after the inception of unstable boiling. It is important to note that the ratios of the spectrum peaks show variations more noticeable with mass velocity, whereas the ratios of the mean spectrum on side-lobes of unstable boiling to the mean spectrum on side-lobes stable boiling conditions vary less. As a result, because of its less varying change with mass velocity the latter parameter can be better used to determine the unstable boiling event for various mass velocities.

The pressure fluctuations for devices 2CWUB and 3HWUB are demonstrated in Figs. 7a and b, and Figs. 8 a and b, respectively. As seen from these figures, pressure fluctuations are also minor with respect to average pressure drop in these devices.

b-) Pressure drop demand curves

The dependence of the pressure drop on the effective heat flux provides useful clues to predict boiling inception and CHF condition. It is well documented and explicated in literature that the pressure drop has a minimum at the onset of significant void (OSV) conditions, beyond which the bubbles detaching from the heated channel wall can survive condensation sufficiently to cause bulk voidage (Collier and Thome, 1994). An increase in heat flux beyond the OSV conditions results in an increase in the pressure-drop required to maintain a fixed flow rate.

Figure 9 shows the characteristic pressure demand curves for devices 1CRUB, 2CWUB and 3HWUB. The pressure drop demand for a fixed mass flux moderately declines with heat flux during the single-phase flow, since with the increase in liquid temperature during single-phase flows the liquid viscosity drops, which in turn has a decreasing effect on the required pressure drop to maintain constant flow rate. This decline in pressure drop continues, until the characteristic minimum is reached, and a surge in the void fraction is instigated. Beyond this minimum, two-phase flow is present, and the increase in the void fraction increases the pressure drop demand. The only difference in the profiles between refrigerant and water studies is that a large jump is remarkable in device 1CRUB operated with R-123, whereas the jump is minor for device 2CWUB. This is attributed to the delay in boiling inception for device 1CRUB due to high wetability of R-123 compared to water. After this delay, a rigorous boiling occurs, which leads to a large pressure jump.

To outline more differences between unstable boiling with water and R-123, images of unstable boiling conditions should be investigated to account for the nature of unstable boiling for each case. Figure 10 demonstrates periodic flow patterns of device 1CRUB at G=887 kg/m^{2}s, which had been recorded in the visualization studies along with the time. Figure 10a corresponds to the initiation of boiling, when small bubbles start to form. Active nucleate sites increase with time particularly near the stagnation region of pin fins, where there is no flow and therefore a temperature rise occurs, and the emerging bubbles from pin fin surfaces near the stagnation regions commence to grow as shown in Fig. 10b. The bubbles can be clearly seen in the inlet region on the first column of micro pin fins. The bubbles formed on the surface of micro pin fins, as well as on the surface of the microchannel merge to build vapor slugs, which propagate toward the inlet plenum (Figs. 10c and 10d). These slugs unite to a large slug occupying a significant portion of the inlet region of the device (Fig. 10e). The large slug is then pushed by the drag force against the surface tension forces acting on it (Figs. 10 f,g,h), so that it collapses, and a two-phase mixture travels from the inlet region to the exit of the device. The same series of events occur periodically for each flow rate at the pin fin device 1CRUB.

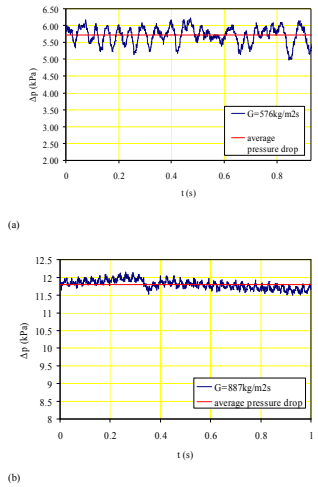

Fig. 3. Pressure fluctuations before unstable boiling conditions for device 1CRUB at a) G=576 kg/m^{2}s and b) G=887 kg/m^{2}s.

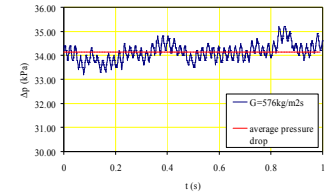

(a)

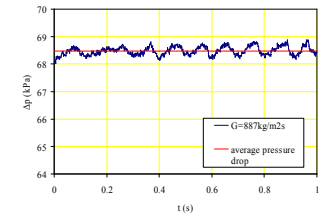

(b)

Fig. 4. Pressure fluctuations before unstable boiling conditions for device 1CRUB at a) G=576 kg/m^{2}s and b) G=887 kg/m^{2}s.

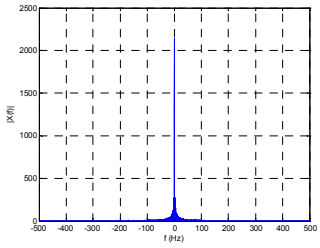

(a) G=329 kg/m^{2}s

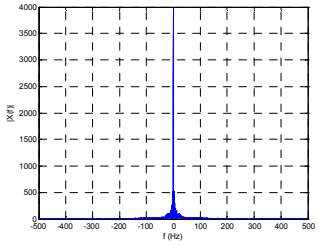

(b) G=576 kg/m^{2}s

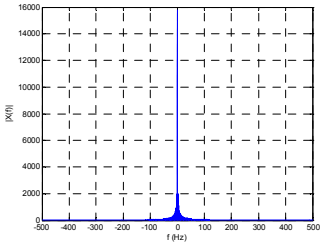

(c) G=887 kg/m^{2}s

Fig. 5. FFT profiles before the unstable boiling

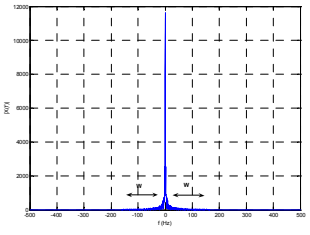

(a) G=329 kg/m^{2}s

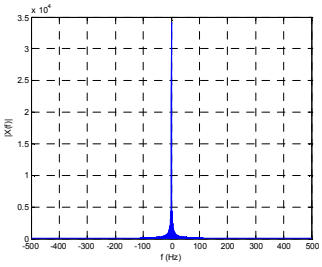

(b) G=576 kg/m^{2}s

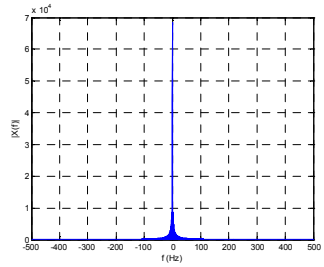

(c) G=887 kg/m^{2}s

Fig.6. FFT profiles after the unstable boiling

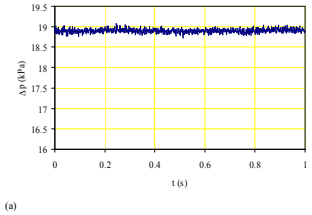

(a)

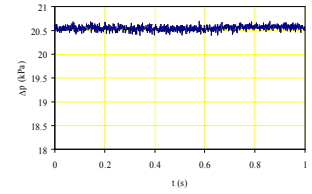

(b)

Fig. 7. Pressure fluctuations a) before and b) after unstable boiling conditions for device 2CWUB at G=1033 kg/m^{2}s.

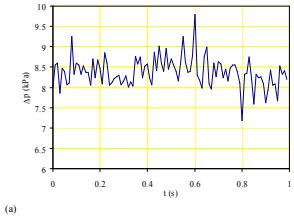

(a)

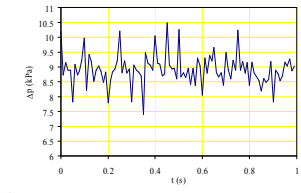

(b)

Fig. 8. Pressure fluctuations a) before and b) after unstable boiling conditions for device 3HWUB at G=1033 kg/m^{2}s.

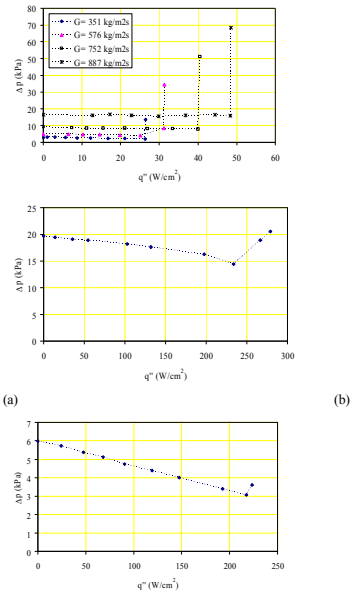

Fig. 9. Pressure drop demand curves for devices a) 1CRUB, b) 2CWUB and c) 3HWUB.

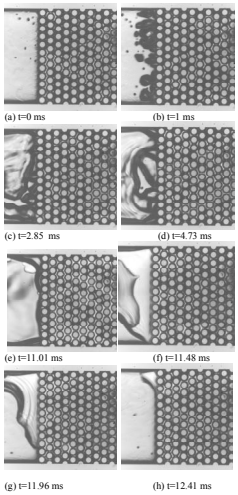

Fig. 10. Unstable boiling images recorded for device 1CRUB.

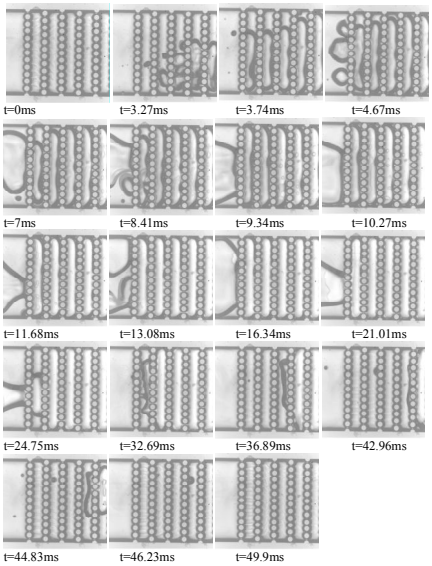

Fig. 11. Unstable boiling images recorded for device 2CWUB (G=1033 kg/m^{2}s).

The flow patterns are similar for water compared to the refrigerant as shown in Fig. 11, which consists of unstable boiling images taken for device 2CWUB. The major difference lies in the surface superheat at the boiling inception, which is much higher for the refrigerant. The main reason can be attributed to better wetability characteristics of R-123 so that all of the larger surface cavities may be flooded with the result that a high superheat is required for nucleation as discussed in the previous section [Koşar and Peles (2006a)]. Once boiling incepts boiling vapor burst instabilities are initiated, a sudden appearance and rapid growth of the vapor phase in liquid were observed, and high values of superheat wave have been achieved. The explosive-like vapor growth seems to be periodic in nature with respect to the visualization study (with a period of 12.41 ms). Koşar and Peles (2006a) associated the corresponding instability with chugging, which is a static instability mode in conventional channels. For water, however, no high superheats are required for boiling inception. After the formation of a large volume of slug in the inlet region moving toward the inlet plenum of device 2CWUB, the flow pushes the slug in a much longer time (~32 ms) compared to the refrigerant boiling flow in device 1CRUB. The instabilities observed with water as working fluid may be linked to high surface tension forces, which provide resistance for bubbles to detach form pin fin surfaces and thus enable them to grow and merge to larger bubbles. The more space the bubbles occupy, the more likely the temperature concentration occurs, which results in a large rise in the average surface temperature. When the flow becomes able to force the slug along the device, liquid replenishment occurs along with a drop in the average surface temperature. As a result, the surface temperature shows a cyclic temperature profile with the cyclic occurrence of flow patterns. These fluctuations in the surface temperature are similar to the refrigerant flow. However, surface tension plays the major role in this case rather than the instabilities for R-123, which have explosive and rapid nature occurrence with much higher frequencies (period$_{R\text{-}123}$=12.43 ms<period$_{water}$=49.9ms).

Stable Boiling

Two-phase pressure drop in micro pin fin configuration leading to stable boiling

The two-phase frictional pressure drop is characterized by a steady and rapid increase with increasing vapor/gas quality and is frequently related to the Martinelli parameter X through the two-phase frictional multiplier, ϕ_L^2, by relationship of the form:

$$\phi_L^2 = 1 + \frac{C}{X} + \frac{1}{X^2} \text{ where } \phi_L^2 = \frac{\Delta p_{2\phi,fr}}{\Delta p_{1\phi,fr}} = \frac{\Delta p_{2\phi,fr}}{\left(\frac{f_L N_{row} G_L^2}{2\rho_L}\right)} \quad (1)$$

where

Liquid laminar, gas laminar $$X_{vv}^2 = \left(\frac{G_L}{G_G}\right)\frac{\rho_G \mu_L}{\rho_L \mu_G} \quad (2)$$

Liquid laminar, gas turbulent $$X_{vt}^2 = \frac{64}{0.184}\left(\frac{G_L}{G_G}\right)\frac{\rho_G \mu_L}{\rho_L \mu_G}\left(\frac{G_G d}{\mu_G}\right)^{-0.8} \quad (3)$$

Liquid turbulent, gas turbulent $$X_{tt}^2 = \left(\frac{G_L}{G_G}\right)^{1.8}\frac{\rho_G}{\rho_L}\left(\frac{\mu_L}{\mu_G}\right)^{0.2} \quad (4)$$

The constant C varies depending on the flow conditions, such that:

C=5 for X_{vv}, C=12 for X_{vt}, and C=8 for X_{tt}

For in-tube two-phase flow the dependency of the two-phase frictional multiplier on the Martinelli parameter takes different forms depending on the flow pattern. Due to the lack of information about C values for tube bundles, C (C=12 for liquid laminar-gas turbulent flow, C=5 for liquid laminar-gas laminar flow) values recommended for channel flow were utilized in the comparison for liquid laminar-gas turbulent and liquid laminar-gas laminar flow, while for liquid turbulent- gas turbulent flow the best fit value of C recommended in the cross flow literature Dowlati and Kawaji (1999) was employed.

Experimental two-phase frictional data as a function of average Martinelli parameters X_{vv}, X_{vt}, and X_{tt} are depicted in Fig. 12a, Fig. 12b, and Fig. 12c along with the C values recommended for channel flow, respectively. In evaluating the Martinelli parameters half of the exit quality was used. This was done to avoid the singularities at x=0 due to the division by zero when integrating two-phase multiplier expressions from zero to exit quality. Thus, half of the exit quality represented the change in the quality from zero to exit quality.

Employing X_{vv} and C value recommended for laminar channel flow for both liquid and vapor phase provides the best prediction of the experimental data to Eq. 1, whereas Eq. 1 significantly overpredicts (more than 30%) the experimental data with respect to the parameters X_{vt}, and X_{tt}. Since the liquid only Reynolds numbers Re_{LO} (Gd/μ_L) ranges from 413 to 976, it is not surprising that laminar flow parameter for both phases is appropriate. Moreover, the good prediction provided by the C value recommended for channel flow suggests that laminar channel flow introduced by micro scale has a more dominant effect on the pressure drop than the effects of pin fins placed inside the channel in micro scale.

Schrage et al. (1988) developed two-phase frictional multiplier correlations based on the dominant flow pattern. Similar to their results, the effect of flow pattern on frictional multiplier is also evident in the current study (Fig. 13a). The data associated with spray-annular flow pattern (X_{vv} less than ~2) fall with ±30% of the theoretical prediction, while the trends of the experimental data for the wavy-intermittent and bubbly flows are different from those of spray-annular flow, and the predictions of the theoretical results are poor. This could be explained by the distinct and clear separation between the liquid and vapor phases in spray-annular flow. Both phases are well separated by well-defined boundaries, which suits very well to the separated flow assumption in the Lockhart and Martinelli model (1949). However, for bubbly and wavy-intermittent flows the phase velocities are similar, and the boundaries between the phases are less identifiable compared to the spray-annular flow and change with time unlike spray-annular flow. As a consequence, there are significant deviations in experimental data from the theoretical prediction for bubbly and wavy-intermittent flows. This suggests that, similar to Schrage et al. (1988), the two-phase frictional multiplier should be correlated in conjunction of the flow patterns.

Another interesting feature of Figs. 13a, 13b, and 13c is that the transition from one flow pattern to another occurs at similar X_{vv} value for all mass velocities. The line $X_{vv}\approx1.8$ constitutes the boundary between spray-annular flow and wavy-intermittent flow, while the line $X_{vv}\approx3$ separates bubbly flow from wavy-intermittent flow. Thus, it can be concluded that the Martinelli parameter is an important parameter dictating flow morphology transition. Low values of X_{vv} correspond to spray-annular flow, whereas high values of X_{vv} suggest bubbly flow. It can be also observed that the two-phase frictional multipliers corresponding to spray-annular flow are greater than for other flow patterns. This suggests that the ratio between two-phase frictional pressure drop and single-phase pressure drop is greater for spray-annular flow. The high slip ratio between the vapor-phase with high superficial velocity and nearly stationary thin liquid film around micro-pin fins as well as high void fractions in spray-annular flows are responsible for higher two-phase frictional multiplier values.

Three different C_1 and C_2 values (Table 3) are derived based on X_{vv} to provide the best curve fit for the experimental data corresponding to each flow pattern in the following form, similar to Schrage et al. (1988):

$$\phi_L^2 = 1 + \frac{C_1}{X} + \frac{C_2}{X^2} \qquad (13)$$

The resulting mean absolute errors (MAE) are 5.4%, 27.5%, and 30.2% for bubbly, wavy-intermittent and spray-annular flow, respectively. As seen in Fig. 14 most all of the experimental data are predicted within ±30% for X_{vv} values ranging from 0.7 to 37.2 using the recommended C_1 and C_2 values in Table 3.

FLOW PATTERN	C_1	C_2	MAE (%)
Bubbly $X_{vv}<1.8$	1.24	-3.26	5.4
Wavy-intermittent $1.8<X_{vv}<3$	-7.79	19.95	27.5
Spray-annular $X_{vv}>3$	3.22	5.33	30.2

Table 3. C_1 and C_2 values providing the best curve fit for the experimental data based on X_{vv}.

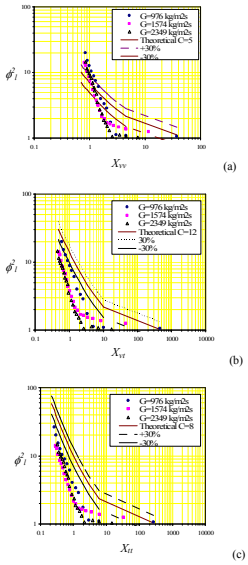

Fig. 12. Experimental two-phase frictional multiplier data as a function of (a) X_{vv}, (b) X_{vt} and (c) X_{tt} and the theoretical predictions.

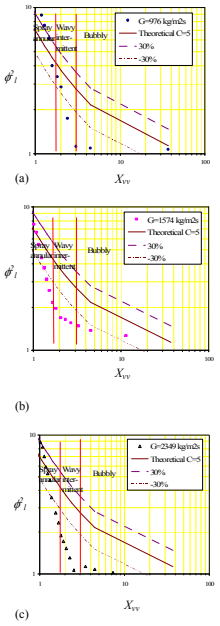

Fig. 13. Experimental two-phase frictional multiplier data as a function of X_{vv} at (a) G=976 kg/m^{2}s, (b) G=1574 kg/m^{2}s, and (c) G=2349 kg/m^{2}s.

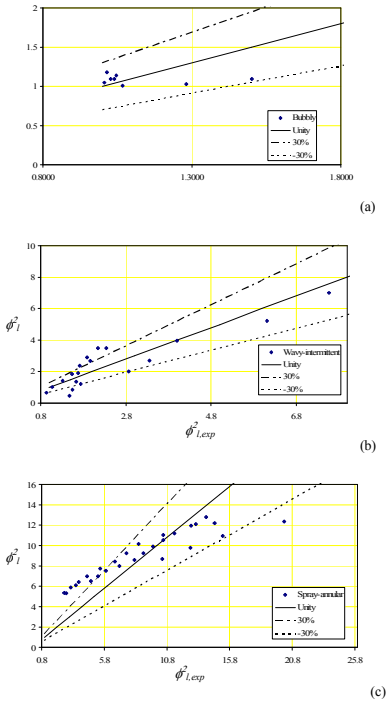

Fig. 14. Theoretical predictions with C values in Table 2 for (a) Bubbly flow, (b) Wavy-intermittent flow, and (c) Spray-annular flow.

CONCLUSIONS

In this study, two-phase pressure drop has been studied in micro pin fin heat sinks. Pressure signals and flow images were provided for unstable boiling conditions obtained from three of the devices and leading to severe temperature fluctuations and flow instabilities. For stable boiling conditions, two-phase frictional multipliers have been evaluated in the light of the flow patterns observed in this study and have been compared to the theoretical predictions for conventional tube bundles. The main conclusions drawn from this study are:

For unstable boiling:

- A meager increase in heat flux triggers an abrupt and intense boiling with considerable increase in the surface temperature and pressure drop marking the arrival of flow instabilities at boiling inception.
- There are no significant pressure fluctuations with the respect to time averaged pressure drop before and after unstable boiling initiates, and peak to peak pressure drop fluctuations remain small compared to the time averaged pressure drop, which is in contrast to the (Critical Heat Flux) CHF condition in microchannels in parallel. However, a drastic change is observed in the pressure signals with the initiation of unstable boiling, and a sharp increase in the magnitude peaks of the FFT profiles is apparent. Moreover, not only the spectrum peak increases significantly but the side-lobe energy also gets drastically higher after the inception of unstable boiling.
- The surface temperature shows a cyclic temperature profile with the cyclic occurrence of flow patterns. These fluctuations in the surface temperature are similar for both water and the refrigerant flow. However, surface tension plays the major role in this case rather than the instabilities for R-123, which have explosive and rapid nature occurrence with much higher frequencies.

For stable boiling:

- Three different flow patterns are detected in flow visualization studies, which are bubby, wavy-intermittent, and -annular flow patterns.
- The Martinelli parameter Xvv recommended for laminar flow for both liquid and vapor phase is found to be the suitable parameter for representing the experimental two-phase frictional multiplier data by the theory.
- The experimental two-phase frictional multiplier is strongly dependent on the flow pattern. The data corresponding to spray-annular flow could be correlated better by the theory compared to bubbly and wavy-intermittent flow.
- The Martinelli parameter Xvv is a crucial parameter for the characterization of the flow pattern. The transition from a particular flow pattern to another occurs at about the same X_{vv} value (X_{vv}≈1.8 for the bubbly flow to wavy-intermittent flow, X_{vv}≈3 for wavy-intermittent to spray annular flow) over the mass velocity range of this study.

REFERENCES

1. S.S. Mehendale, A.M. Jacobi, and R.K. Shah, Fluid flow and heat transfer at micro- and meso-scales with application to heat exchanger design, *Applied Mechanics Review,* vol. 53, pp. 175-193, 2000.
2. B. Palm, Heat transfer in microchannels, *Microscale Thermophysical Engineering*, vol. 5, pp. 155-175, 2001.
3. S.G. Kandlikar, Two-phase flow patterns, pressure drop, and heat transfer during boiling in minichannels flow

passages of compact evaporators, *Heat Transfer Engineering*, vol. 23, pp. 5-23, 2002.
4. A.E. Bergles, J.H. Lienhard, G.E. Kendall, and P. Griffith, Boiling and evaporation in small diameter channels, *Heat Transfer Engineering*, vol. 24, pp. 18-40, 2003.
5. S.V. Garimella and V. Singhal, Single-phase flow and heat transport and pumping considerations in microchannel heat sinks, *Heat Transfer Engineering*, vol. 25, pp. 15-25, 2004.
6. S.G. Kandlikar and W.J. Grande, Evaluation of single-phase flow in microchannels for high heat flux chip cooling - thermohydraulic performance enhancement and fabrication technology, *Heat Transfer Engineering*, vol. 25, pp. 5-16, 2004.
7. J.R. Thome, Boiling in micro channels: a review of experiment and theory, *International Journal of Heat and Fluid Flow*, vol. 25, pp. 128-139, 2004.
8. S.G. Kandlikar, Heat transfer mechanisms during flow boiling in microchannels, *Journal of Heat Transfer*, vol. 126, pp. 8-16, 2004.
9. E.G. Colgan, B. Furman, M. Gaynes, W. Graham, N. LaBianca, J.H. Magerlein, R.J. Polastre, M.B. Rothwell, R.J. Bezama, R. Choudhary, K. Marston, H. Toy, J. Wakil, J. Zitz, and R. Schmidt, A practical implementation of silicon microchannel coolers for high power chips, *21st IEEE SEMI-THERM Symposium*, San Jose, CA, March 15-17, 2005.
10. W. Qu, F. Pfefferkorn, and Y. Jeon, Experimental study of single-phase flow and heat transfer in micro-pin-fin and micro-channel heat sinks, *ASME International Mechanical Engineering Congress and Exposition*, November 5-12, Orlando, Florida, 2005, IMECE2005-80557.
11. R.S. Prasher, J. Dirner, J.-Y. Chang, A. Myers, D. Chau, D. He, and S. Prstic, Nusselt number and friction factor of staggered arrays of low aspect ratio micro pin fins under cross flow, *Journal of Heat Transfer*, vol. 129, pp. 141-153, 2007.
12. A. Koşar and Y. Peles, Convective flow of refrigerant (R-123) across a bank of micro pin fins, *International Journal of Heat and Mass Transfer*, vol. 49, pp. 3142-3155, 2006a.
13. A. Koşar and Y. Peles, Thermal-hydraulic performance of MEMS-based pin fin heat sink, *Journal of Heat Transfer*, vol. 128, pp.131-131, 2006b.
14. A. Koşar and Y. Peles, Boiling heat transfer in a hydrofoil-based micro pin fin heat sink, *International Journal of Heat and Mass Transfer,* vol. 50, pp. 1018-1034, 2007.
15. I.D.R. Grant and D. Chisholm, Two-phase flow on the shell-side of a segmentally baffled shell-and-tube heat exchanger, *Journal of Heat Transfer*, vol. 101, pp. 38-42, 1979.
16. D.S. Schrage, J.-T. Hsu, and M.K. Jensen, Two-phase pressure drop in vertical crossflow across a horizontal tube bundle, *American Institute of Chemical Engineers Journal*, vol. 34, pp. 107-115, 1988.
17. R. Dowlati, M. Kawaji, Two-phase flow and boiling heat transfer in tube bundles, *Handbook of Phase Change: Boiling and Condensation,* Taylor&Francis, Ann Arbor, Chapter 12, 1999.
18. R. Dowlati, M. Kawaji, and A.M.C. Chan, Two-phase crossflow and boiling heat transfer in horizontal tube bundles, *Journal of Heat Transfer*, vol. 118, pp. 124-131, 1996.
19. R. Dowlati, M. Kawaji, and A.M.C. Chan, Pitch-to-diameter effect on two-phase flow across an in-line tube bundle, *American Institute of Chemical Engineers Journal*, vol. 36, pp. 765-772, 1990.
20. G.P. Xu, K.W. Tou, and C.P. Tso, Two-phase void fraction and pressure drop in horizontal cross flow across a tube bundle, *Journal of Fluid Engineering*, vol. 120 pp. 140-145, 1998.
21. S. Krishnamurthy and Y. Peles, Gas-liquid two-phase flow across a bank of micro pillars, *Physics of Fluids*, vol. 19, 043302- 043302 -14, 2007.
22. S. Kline, F.A. McClintock, Describing uncertainties in single-sample experiments, *Mechanical Engineering*, vol. 75, pp. 3-8, 1953.
23. G.R. Noghrehkar, M. Kawaji, A.M.C. Chan, Investigation of two-phase flow regimes in tube bundles under cross-flow conditions, *International Journal of Multiphase Flow*, vol. 25, pp. 857-874, 1999.
24. R.W. Lockhart and R.C. Martinelli, Proposed correlation of data for isothermal two-phase two-component flow in pipes, *Chemical Engineering Progress*, vol. 45, pp. 39-48, 1949.
25. J.G. Collier and J.R. Thome, Convective Boiling and Condensation, 3rd ed., Oxford University Press, Oxford, pp. 193–195, 1994.